



Huang T. (2024). Prediction ability analysis of phenomenological strength criteria for composites. *Journal of Engineering Sciences (Ukraine)*, Vol. 11(1), pp. D54–D65. [https://doi.org/10.21272/jes.2024.11\(1\).d7](https://doi.org/10.21272/jes.2024.11(1).d7)

Prediction Ability Analysis of Phenomenological Strength Criteria for Composites

Huang T. ^[0009-0001-0972-043X]

National Technical University of Ukraine “Igor Sikorsky Kyiv Polytechnic Institute”, 37, Peremohy Ave., 03056 Kyiv, Ukraine

Article info:

Submitted: October 4, 2023
 Received in revised form: February 12, 2024
 Accepted for publication: March 7, 2024
 Available online: March 18, 2024

*Corresponding email:

t.khuan@kpi.ua

Abstract. The article examines and assesses the phenomenological strength theory of composite materials. A comparative analysis of the theoretical envelopes was conducted for each criterion. A unified form of the phenomenological strength criterion was established. The study specifically examined the effects of altering the interaction parameter on the Tsai-Wu criterion’s theoretical envelope. Based on the available experimental data, the study plotted the failure envelopes of each strength criterion under planar composite stress states. The variation of these envelopes across various stress quadrants was highlighted. As a result of the examinations, four typical phenomenological strength criteria were chosen. The composites’ off-axis tensile and biaxial loading test data were used to evaluate the predictive power objectively. The results showed that not all stress states’ test results agreed with the predictions of the phenomenological strength theory. The criterion proposed by Norris and Tsai-Hill performed better at accounting for the material’s different compressive and tensile characteristics. The other criteria tended to be conservative under particular circumstances. Simultaneously, the Hoffman criterion matched the test data more closely over a broader range of stress states. Overall, this study clarified the limitations and applicability of various strength criteria in composite material strength prediction.

Keywords: composite materials, tensile compression test, failure envelope, strength prediction.

1 Introduction

Composite materials are widely used in aerospace, aviation, transportation, electronics, energy, and other fields due to their excellent properties, which include a high strength-to-weight ratio and high modulus ratio. These materials offer high dimensional stability, design flexibility, and excellent mechanical properties [1]. This makes it possible to adapt structural design to specific operating environments and broadens its applications.

For instance, the primary load-bearing structures of the Airbus A380 and Boeing 787, such as their fuselages and wing girders, are made of composite materials. This improves the aircraft’s mechanical characteristics while drastically lowering structural weight and fuel consumption. In particular, the Boeing 787 uses 50 % more composite materials than the A380, which uses 20 % more [2].

Single-ply laminated structure failure behavior and theory are typically assessed in application analysis of composite materials.

This method compares the ultimate strength or strain of the single-ply laminate with each ply’s stress or strain state. In composite strength, the primary methodology used is phenomenological failure criteria. From the yield criteria for isotropic materials, phenomenological failure criteria were created. These include a variety of polynomial and tensor criteria, which define the damaged surface by describing the material strength as a function of the material strength using mathematical expressions. Given the deficiencies in the existing literature concerning the evaluation of the phenomenological strength theory of composite materials, an objective assessment of their properties had to be provided.

The phenomenological strength criteria are first formally unified in this article. Next, based on test data from the literature, the failure envelopes fitted to each strength criterion under plane stress states are established.

Finally, the predictive ability of each strength criterion is analyzed objectively using multiple sets of composite test data.

2 Literature Review

The failure criteria for composite materials based on phenomenology are developed by focusing on the macroscopic stress-strain behavior of the material rather than detailed microstructural analysis or specific failure mechanisms. The overall state of the composite material is represented by a uniform polynomial or other comparable mathematical expression in these criteria.

Failure is thought to occur when the material's stress or strain state approaches or surpasses a critical threshold indicated by these expressions. Phenomenological failure criteria have the benefit of being straightforward and universal. These criteria make it possible to quickly evaluate a material's overall performance through holistic mathematical models, which is especially helpful in the early phases of engineering design and analysis.

While they may not consistently predict specific failure modes or account for complex interactions within a material's microstructure, their ease of use and quick insight into material behavior under different loading conditions keep these standards widely favored for numerous practical applications [3]. According to the phenomenological strength criterion, the failure of a composite material is defined as the strain or stress component reaching its corresponding strength limit (or destructive strain) in any of the principal directions. This criterion clearly distinguishes failure modes but ignores how the various stress components interact.

The Norris strength criterion [4] includes a term for positive stress interactions to increase the criterion's prediction accuracy. The Tsai-Hill strength criterion [5] is an orthotropic anisotropic application of the Von Mises yield criterion for isotropic materials. This criterion applies to composite materials with equal tensile and compressive strength properties and considers the interaction of stresses in the three main directions.

The Hoffman strength criterion [6], based on the Tsai-Hill criterion, adds a stress primary term and distinguishes between longitudinal and transverse tensile and compressive strengths. This distinction considers the influence of the variation in tensile and compressive strengths on material damage.

Tsai and Wu proposed the Tsai-Wu strength criterion to offer a cohesive theoretical framework in the tensor form [7].

According to this criterion, the stress secondary term creates a smooth elliptical failure envelope, while the primary term represents the difference between the tensile and compressive strength properties.

Based on this, several strength criteria were later revised and created. The Tsai-Wu tensor criterion gains a tertiary term from the Wu-Scheublein criterion [8]. Except for providing a value for the strength factor F_{12} , the Cowin criterion [9] is comparable to the Tsai-Wu criterion. A primary term for positive stress, a secondary term for shear stress, and a positive-stress interaction term using the Yeh-Stratton criterion [10].

Arruda [11] has developed new methods using the Tsai-Wu model that allow the implementation of the classical intrinsic law of damage evolution based on the regularisation of the fracture energy and implemented it in the commercial finite element software ABAQUS using the user-defined material (UMAT) subroutine.

The fractional quadrant (stress plane) describes the failure envelope space, the quadratic term of the positive stress, and the positive stress interaction term. In a recent research, Li [12] re-examined the quadratic function of the failure criterion for composites. Analyzing the nature of the quadratic failure function in the context of analytical geometry enhances the consistency of the failure criterion based on it. However, these criteria are frequently not widely adopted because of their intricate form and requirement for many fitting parameters.

Apart from the fundamental, ultimate strength criterion (maximum stress/strain criterion), composite materials' most commonly applied phenomenology-based failure criteria are the Tsai-Wu, Hoffman, Tsai-Hill, and Norris criteria. Each of these failure theories has distinct features and limitations. These four phenomenological strength criteria were chosen for the analysis.

3 Research Methodology

3.1 Phenomenological strength criterion

Given the polynomial nature of the expressions of the phenomenological strength criteria, the expressions of the phenomenological strength criteria are written in a uniform form similar to the Tsai-Wu criterion, and the interaction parameter of the polynomial forms of the four phenomenological strength criteria involved in the evaluation and analysis can be listed in Table 1.

Table 1 – Phenomenological strength criteria

Strength criteria	F_1	F_2	F_{11}	F_{22}	F_{66}	F_{12}
Norris [4]	0	0	$\frac{1}{X^2}$	$\frac{1}{Y^2}$	$\frac{1}{S_{12}^2}$	$-\frac{1}{XY}$
Tsai-Hill [5]	0	0	$\frac{1}{X^2}$	$\frac{1}{Y^2}$	$\frac{1}{S_{12}^2}$	$-\frac{1}{X^2}$
Hoffman[6]	$\frac{1}{X_t} - \frac{1}{X_c}$	$\frac{1}{Y_t} - \frac{1}{Y_c}$	$\frac{1}{X_t X_c}$	$\frac{1}{Y_t Y_c}$	$\frac{1}{S_{12}^2}$	$-\frac{1}{X_t X_c}$
Tsai-Wu [7]	$\frac{1}{X_t} - \frac{1}{X_c}$	$\frac{1}{Y_t} - \frac{1}{Y_c}$	$\frac{1}{X_t X_c}$	$\frac{1}{Y_t Y_c}$	$\frac{1}{S_{12}^2}$	$F_{12}^* \sqrt{F_{11} F_{22}}$

3.2 Theoretical failure envelope

The first two strength criteria have no stress primary terms in their polynomial equations, whereas the last two strength criteria incorporate the effect of primary terms and account for the difference in the materials' tensile and compressive strengths. The main difference between the criteria without primary terms and those with primary terms is the value of the interaction parameter F_{12} .

The physical properties and differences of various phenomenological strength criteria are investigated by developing theoretical damage envelopes for a variety of stress state combinations and extending them to three-dimensional stress states. The theoretical modeling allows for an objective exploration of the physical properties revealed by each criterion through careful comparison and analysis of the strength damage criteria. This method not

only improves understanding of the applicability and limitations of each criterion, but it also lays the theoretical groundwork for predicting and optimizing material strength.

In a plane stress condition, failure envelopes for different strength criteria under different stress states ($\sigma_1 - \sigma_2$, $\sigma_1 - \tau_{12}$, and $\sigma_2 - \tau_{12}$) were found using data on AS4/PEEK laminate material properties from source [13].

The stress ratios in each principal direction are plotted against the corresponding tensile (X_t , Y_t) or shear strength (S_{12}) to represent these envelopes as dimensionless stresses. The Tsai-Wu criterion [14–18] adopts the value of F_{12} [1919] in accordance with Tsai and Hahn's recommendation, which is $F_{12} = -\sqrt{F_{11}F_{22}}/2$.

The basic mechanical properties of AS4/PEEK monolayers are shown in Table 2.

Table 2 – engineering elastic constants and strength values of AS4/PEEK material

Elastic constants	E_1 , GPa	E_2 , GPa	G_{12} , GPa	ν_{12}	ν_{21}
	140.35	9.44	5.403	0.253	0.023
Strength values	X_t , MPa	X_c , MPa	Y_t , MPa	Y_c , MPa	S_{12} , MPa
	2128.0	954.6	93.0	205.9	133.0

Based on fitting different phenomenological strength criteria on the $\sigma_1 - \sigma_2$ stress plane (with $\tau_{12} = 0$), the theoretical failure envelope for AS4/PEEK material is shown in Figure 1.

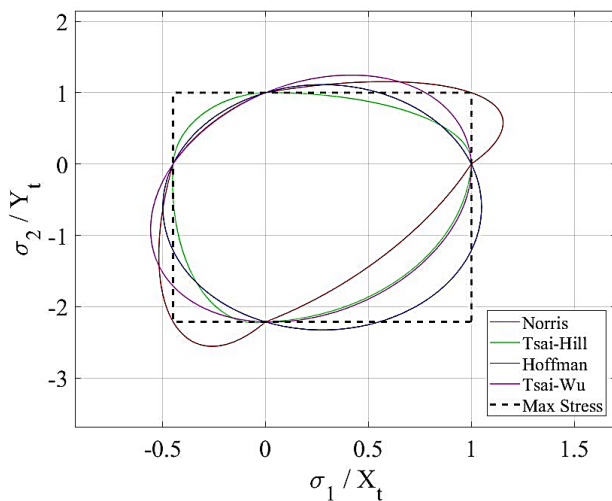


Figure 1 – Failure envelope for each strength criterion for the $\sigma_1 - \sigma_2$ stress state ($\tau_{12} = 0$)

The material's true tensile and compressive strengths are integrated into the corresponding stress quadrants of strength models that ignore the material's unique tensile

and compressive properties (i.e., lack key terms in their equations), improving the assessment of characteristics and predictive precision. The analysis reveals:

1) the envelope of the polynomial strength criterion crosses the coordinate axes four times under uniaxial loading, revealing the material's basic compressive and tensile strengths in both longitudinal and transverse directions;

2) the differences in compressive and tensile strengths are taken into account by the Norris and Tsai-Hill criteria, which produce unique curve equations for various stress quadrants and non-standard elliptical envelope shapes;

3) the interaction parameter F_{12} largely influences the elliptical failure envelopes of Hoffman's and Tsai-Wu's criteria, which have major axes that span the first and third quadrants.

A consistent pattern emerges from the analysis of how different shear stresses τ_{12} affect the material's strength criterion: The failure envelope progressively contracts towards the coordinate center for each phenomenological strength criterion as τ_{12} increases.

Figure 2 illustrates this observation by plotting the failure envelopes for various τ_{12} values (0, 0.25 S_{12} , 0.50 S_{12} , and 0.75 S_{12}) for each criterion.

According to this pattern, higher shear stresses appear to hasten the material's failure process, reducing its strength and raising the risk of failure.

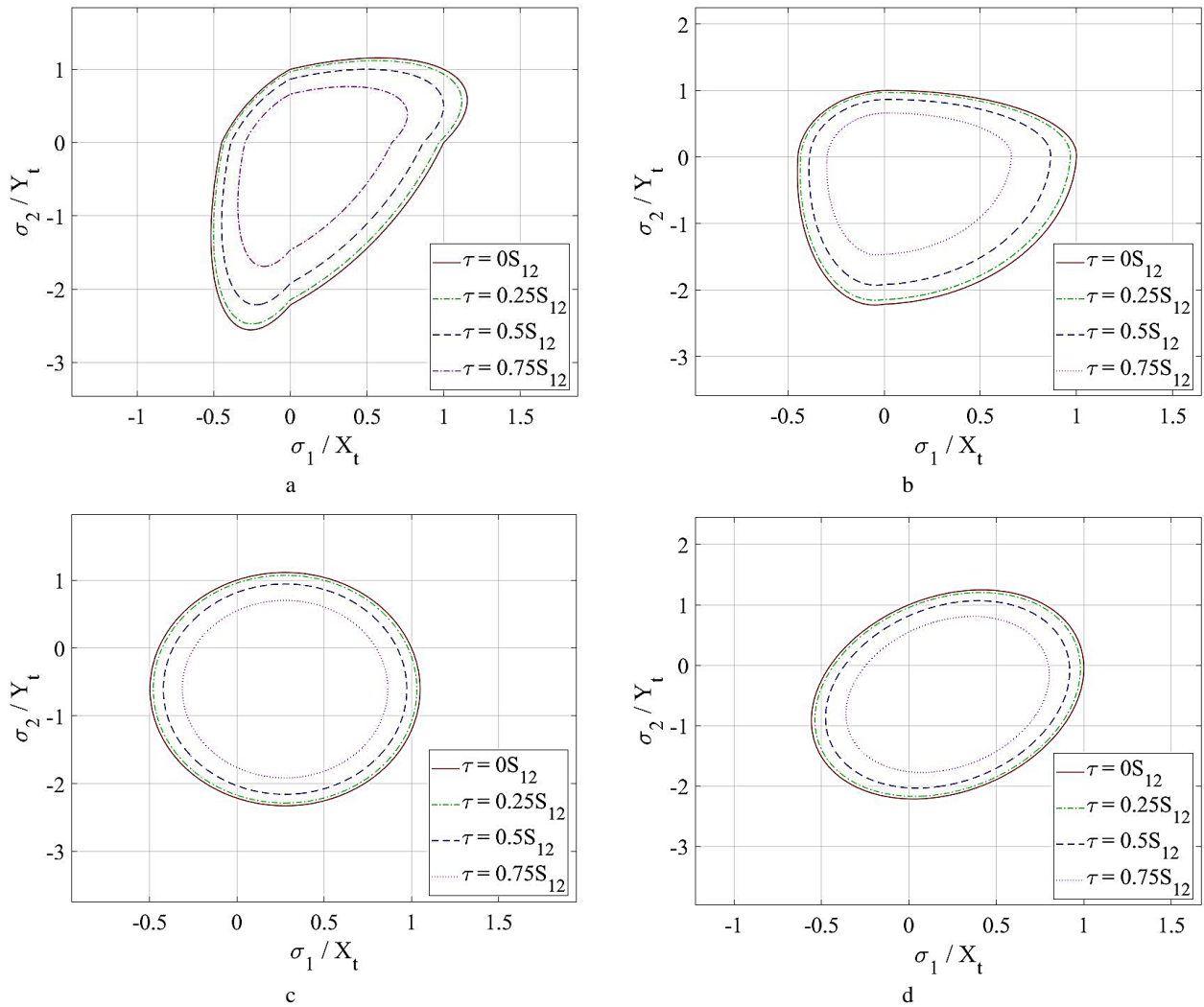


Figure 2 – Failure envelope for each strength criterion in the σ_1 - σ_2 stress plane for different τ_{12} :
a – Norris criterion; b – Tsai-Hill criterion; c – Hoffman criterion; d – Tsai-Wu criterion

Figure 3 illustrates the failure envelopes corresponding to each strength criterion in the σ_1 - τ_{12} stress state ($\sigma_2 = 0$).

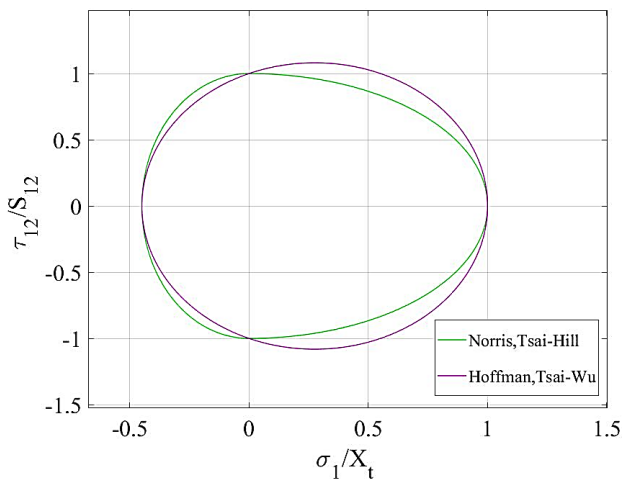


Figure 3 – Failure envelope for each strength criterion for the σ_1 - τ_{12} stress state ($\sigma_2 = 0$)

This figure leads to several conclusions:

1) on the coordinate axis, the failure envelopes for every criterion cross at the exact location;

2) because σ_2 is zero, the positive stress interaction term on the σ_1 - τ_{12} stress plane is null ($F_{12} \sigma_1 \sigma_2 = 0$). The strength criteria equations with and without the primary term exhibit different features: the equations are identical in the absence of the primary term (Norris, Tsai-Hill) and produce perfectly overlapping failure envelopes; the equations are identical in the presence of the primary term (Hoffman, Tsai-Wu) and produce overlapping failure envelopes;

3) the failure envelope for criteria with a primary term forms an elliptical curve, whereas it does not form an elliptical curve without the primary term. This discrepancy results from using different equations to represent failure envelopes in various stress quadrants, which reflects the variations in the compressive and tensile properties of the materials. However, these envelopes resemble parts of an elliptic curve to some extent;

4) the failure envelope of the strength criterion with the primary term extends beyond the $[-S_{12}, S_{12}]$ shear stress

range due to the presence of the σ_1 primary term in the criterion equation. On the other hand, this range is still covered by the envelope without the primary term.

The principal directional stresses σ_2 ($0, 0.25 Y_t, 0.50 Y_t$, and $0.75 Y_t$) that vary with time were examined to

determine the failure envelopes of each strength criterion on the σ_1 - τ_{12} stress plane.

Figure 4 shows the gradient failure envelopes for each criterion.

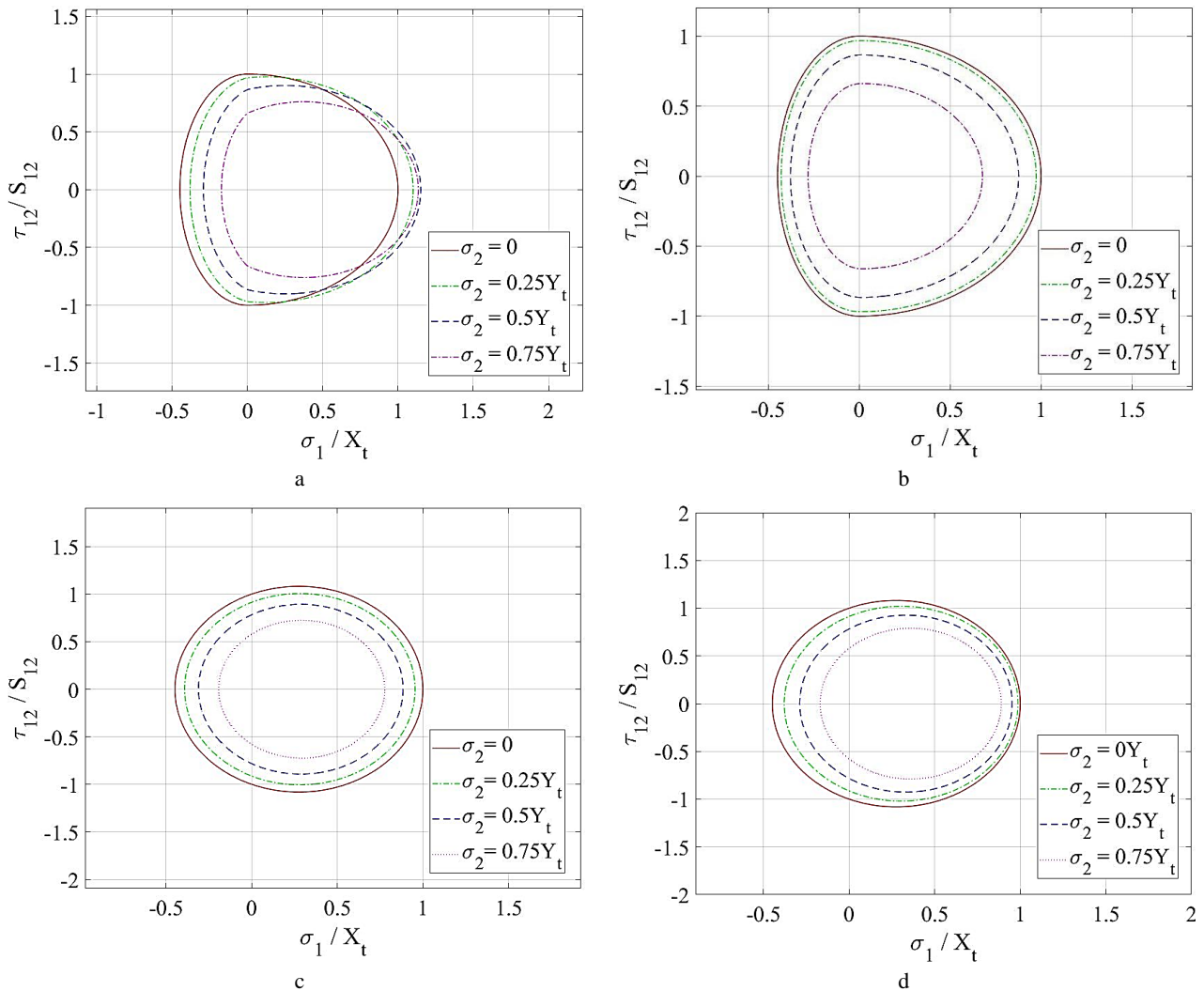


Figure 4 – Failure envelope for each strength criterion in the σ_1 - τ_{12} stress plane for different σ_2 :
 a – Norris criterion; b – Tsai-Hill criterion; c – Hoffman criterion; d – Tsai-Wu criterion

The figure analysis indicates that the failure envelopes, which are defined by the strength criteria, exhibit different levels of convergence towards the coordinate center as σ_2 increases. This suggests that σ_2 increases the likelihood of material failure; the failure envelopes of the criterion without a primary term are grouped on the $\sigma_1 < 0$ side, whereas the Tsai-Wu criterion, which includes a primary term, is grouped on the $\sigma_1 > 0$ side; both the Tsai-Wu and the Norris criteria, with strength parameter Y_t , surpass the material's basic strength range at $\sigma_1 > 0$ in the F_{12} term before reverting to it, suggesting their possible application in ultimate strength design under particular circumstances.

The analysis reveals that:

1) all strength criteria's failure envelopes intersect at the same point on the coordinate axes;

2) given that the positive stress interaction term is zero ($F_{12}\sigma_1\sigma_2 = 0$), the failure envelopes for criteria lacking the primary term align, including the primary term;

3) the failure envelope for the criterion with the primary term forms an elliptic curve. In contrast, the criterion without the primary term deviates from an elliptic curve due to differing equations describing failure envelopes across stress quadrants, reflecting the materials' distinct tensile and compressive properties. However, each quadrant's failure envelope represents a segment of the elliptic curve;

4) influenced by the σ_2 primary term in the criterion equation, the failure envelope for the criterion with the primary term extends beyond the $[-S_{12}, S_{12}]$ shear stress range, unlike the envelope for the criterion without the primary term.

Figure 5 presents the failure envelopes for various strength criteria under the σ_2 - τ_{12} stress state ($\sigma_1 = 0$).

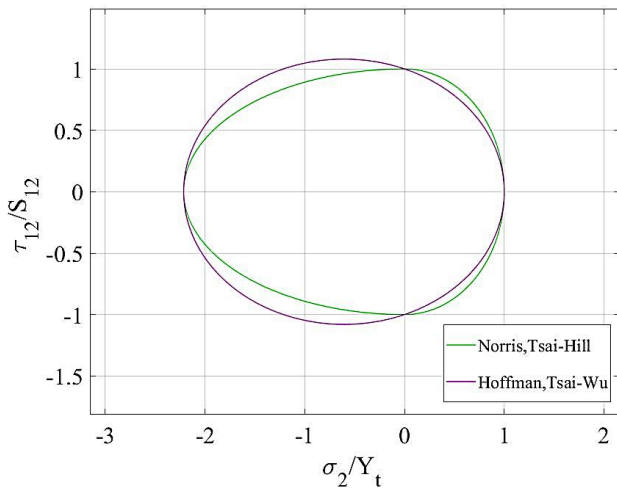


Figure 5 – Failure envelope for each strength criterion for the σ_2 - τ_{12} stress state ($\sigma_1 = 0$)

The failure envelopes of various strength criteria, influenced by differing principal directional stresses σ_1 (0, $0.25 X_t$, $0.50 X_t$, and $0.75 X_t$), were analyzed on the σ_2 - τ_{12} stress plane. The gradient failure envelopes for each criterion are depicted in Figure 6.

Analysis of the figure reveals that the failure envelopes defined by the Norris, Tsai-Hill, and Hoffman criteria exhibit varying extents of convergence towards the coordinate center with increasing σ_1 values. The Norris and Tsai-Wu criteria demonstrate an offset pattern in this convergence; the failure envelopes for the Norris and Tsai-Wu criteria exhibit a distinctive shifted convergence as σ_1 varies, the strength criterion without a primary term shows clustering on the $\sigma_2 > 0$ side, while the Tsai-Wu criterion (with a primary term) exhibits a similar trend.

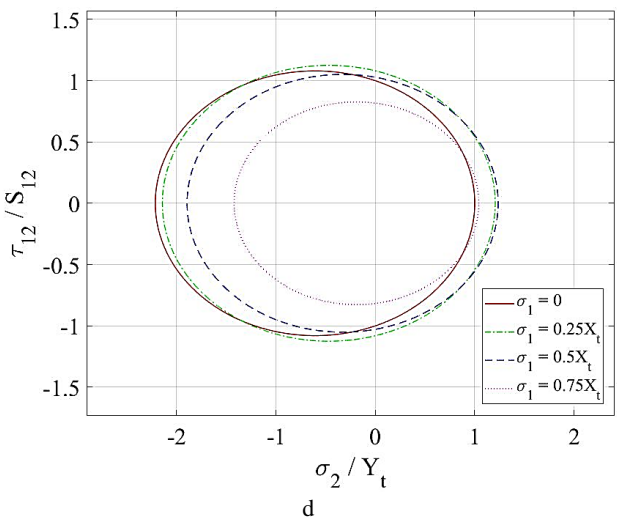
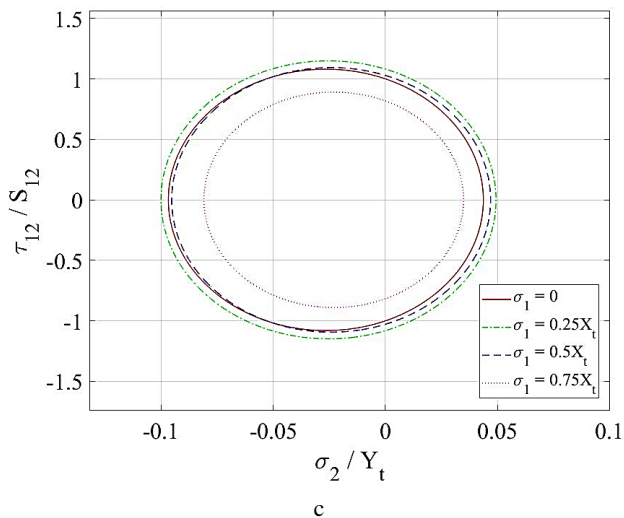
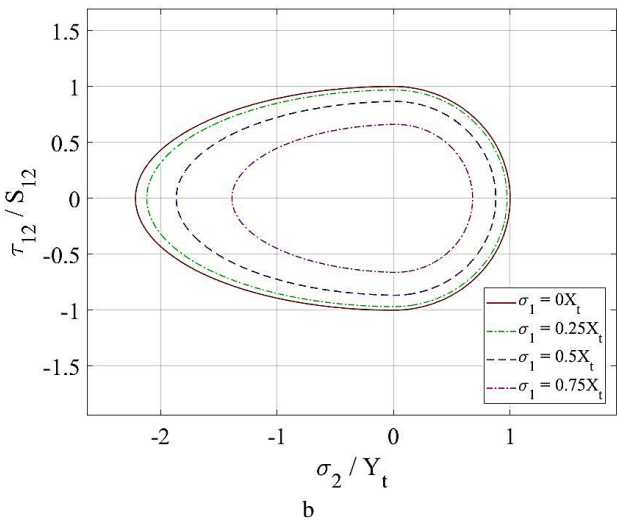
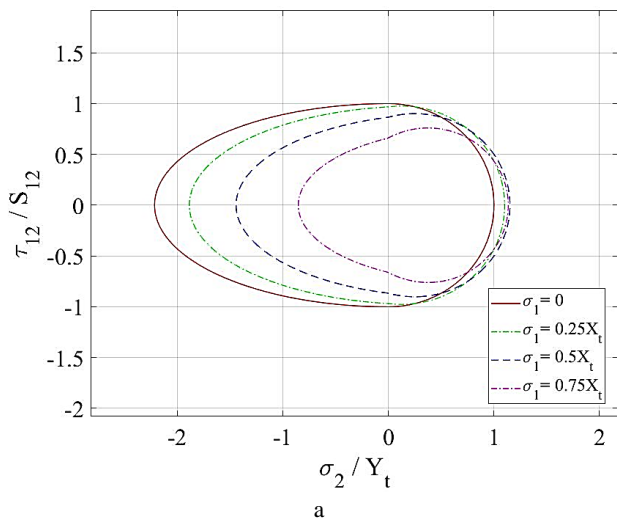


Figure 6 – Failure envelope for each strength criterion in the σ_2 - τ_{12} stress plane for different σ_1 : a – Norris criterion; b – Tsai-Hill criterion; c – Hoffman criterion; d – Tsai-Wu criterion

3.3 Effect of the interaction parameter F_{12} on the failure envelope

As explained above, the interaction parameter F_{12} , (Table 1) is essential for figuring out how much the failure envelope affects and how accurate the predictions are within the strength criterion. This calls for a thorough examination of F_{12} .

A popular model for studying the impact of F_{12} modifications on the failure envelope are the Tsai-Wu criterion, which can be transformed into a variety of polynomial criteria by changing the stress coefficient F_{12} . The interaction parameter F_{12} although widely used in composite material studies, the Tsai-Wu criterion continues to be a focus of research, highlighting the continuous efforts to improve the criterion's accuracy and efficacy.

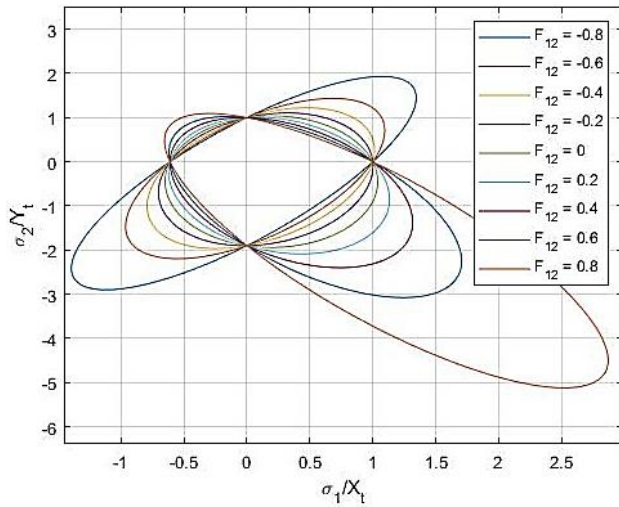


Figure 7 – Effect of different values of F_{12} on the Tsai-Wu criterion failure envelope in the σ_1 - σ_2 stress plane ($\tau_{12} = 0$)

According to Table 1, the dimensionless stress action factor F_{12} was evaluated below unity ($F_{12} < 1$). Seven distinct values of F_{12} ($-0.8, -0.6, -0.4, -0.2, 0, 0.2, 0.4, 0.6,$ and 0.8) were incorporated into the Tsai-Wu criterion to generate corresponding failure envelopes, as depicted in Figure 7, utilizing the AS4/PEEK single-layer from Table 2 (and its strength parameters).

The generated elliptical envelopes always intersect at the same point on the coordinate axes. The ellipses are oriented along the first and third quadrants for values of F_{12} less than zero. As F_{12} decreases, these ellipses become flatter and longer, as indicated by an increasing major axis and a decreasing minor axis. In contrast, the ellipses tilt toward the second and fourth quadrants for F_{12} greater than zero. As F_{12} increases, the ellipses get narrower and extend into the fourth quadrant. Interestingly, the elliptical envelopes gradually surpass the uniaxial fundamental strength values of the material in its principal direction as the absolute value of F_{12} increases.

This pattern indicates that the criterion is making increasingly dangerous predictions, except when biaxial reinforcement increases the material's intrinsic strength.

Therefore, the predictive accuracy of the criterion is highly dependent on the value of F_{12} . Depending on the material properties, F_{12} variations across various stress quadrants must be considered to predict material failure behavior accurately.

3.4 Tensile compression test and analysis

The applicability and feasibility of various strength theories require experimental validation. This section presents a comparative analysis of the predictive capabilities of each strength criterion for internal multiaxial stress states (as demonstrated in off-axis tensile tests) and external multiaxial stress states (as seen in biaxial loading tests), incorporating experimental data from pertinent literature.

When the off-axis tensile stress is σ_x , the magnitude of the stress in each principal direction is:

$$\sigma_1 = \sigma_x \cos^2 \theta, \sigma_2 = \sigma_x \sin^2 \theta, \tau_{12} = \sigma_x \sin \theta \cos \theta. \quad (1)$$

Where θ is the off-axis angle, i.e., the angle between the main direction of the fibers of the specimen and the direction of tensile loading.

Each strength criterion can be expressed in terms of the off-axis tensile stress σ_x and the off-axis angle θ as:

1) the Norris Strength Criteria:

$$\sigma_x^2 \left[\frac{1}{S_{12}^2} \cos^2 \theta \sin^2 \theta + \left(\frac{\cos^4 \theta}{X^2} + \frac{\sin^4 \theta}{Y^2} \right) \right] = 1; \quad (2)$$

2) the Tsai-Hill strength criterion:

$$\sigma_x^2 \left[\frac{1}{S_{12}^2} \cos^2 \theta \sin^2 \theta + \left(\frac{\cos^4 \theta}{X^2} + \frac{\sin^4 \theta}{Y^2} \right) \right] = 1; \quad (3)$$

3) the Hoffman strength criterion:

$$\sigma_x^2 \left[\left(\frac{1}{S_{12}^2} - \frac{1}{X_t X_c} \right) \cos^2 \theta \sin^2 \theta + \left(\frac{\cos^4 \theta}{X_t X_c} + \frac{\sin^4 \theta}{Y_t Y_c} \right) \right] + \sigma_x \left[\frac{X_c - X_t}{X_t X_c} \cos^2 \theta + \frac{Y_c - Y_t}{Y_t Y_c} \sin^2 \theta \right] = 1 \quad (4)$$

4) the Tsai-Wu strength criterion:

$$\sigma_x^2 \left[\left(\frac{1}{S_{12}^2} + 2F_{12} \right) \cos^2 \theta \sin^2 \theta + \left(\frac{\cos^4 \theta}{X_t X_c} + \frac{\sin^4 \theta}{Y_t Y_c} \right) \right] + \sigma_x \left[\frac{X_c - X_t}{X_t X_c} \cos^2 \theta + \frac{Y_c - Y_t}{Y_t Y_c} \sin^2 \theta \right] = 1 \quad (5)$$

As presented in Table 3, the fundamental material property data facilitated the construction of curves depicting theoretical predictions for the off-axis tensile strength according to each strength criterion, varying with the off-axis angle θ . These theoretical outcomes were then juxtaposed with the empirical results from the off-axis tensile tests conducted on the material.

Table 3 – The fundamental material property data

Material	Parameter, MPa				
	X_t	X_c	Y_t	Y_c	S_{12}
AS4/PEEK [13]	2128	93	955	206	93
T800/2500EP [20]	1934	910	49	120	78
Boron/AVCO5505 [21]	1296	2489	62	310	78

4 Results

As shown in Figure 8, the theoretical prediction curves of the off-axis tensile strength of AS4/PEEK laminates using AS4/PEEK laminates are compared with the experimental data.

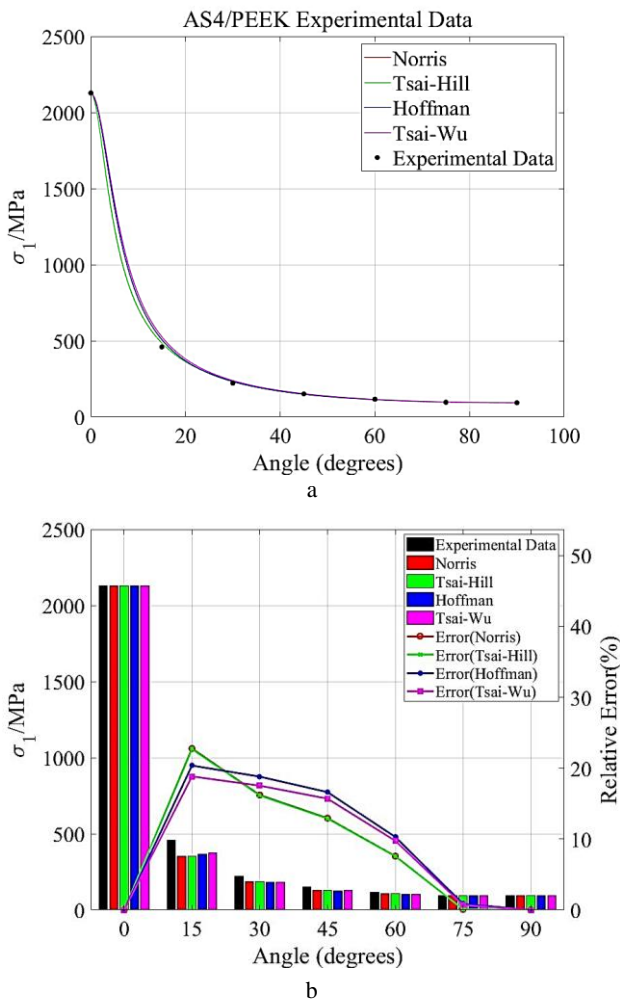


Figure 8 – Comparison of theoretical prediction curves with experimental data: a – approximating curves; b – errors

From Figure 8a, it can be seen that each strength criterion can effectively predict the tensile strength at different off-axis angles θ . The more significant relative errors in the prediction results of the four criteria all appeared at an off-axis angle of 15° and decreased with the increase of the angle.

From Figure 8b, it can be seen that the prediction errors of the Hoffman criterion and the Tsai-Wu criterion were higher than those of the Norris criterion and the Tsai-Hill criterion, with the Tsai-Wu code having the most

significant prediction error at $\theta = 15^\circ$, which was 23 %. For larger off-axis angles (45°, 60°, and 75°), the prediction errors for each criterion were within 20 %.

Figure 9 compares the theoretical prediction of off-axis tensile strength for T800/2500EP laminates and the corresponding experimental data.

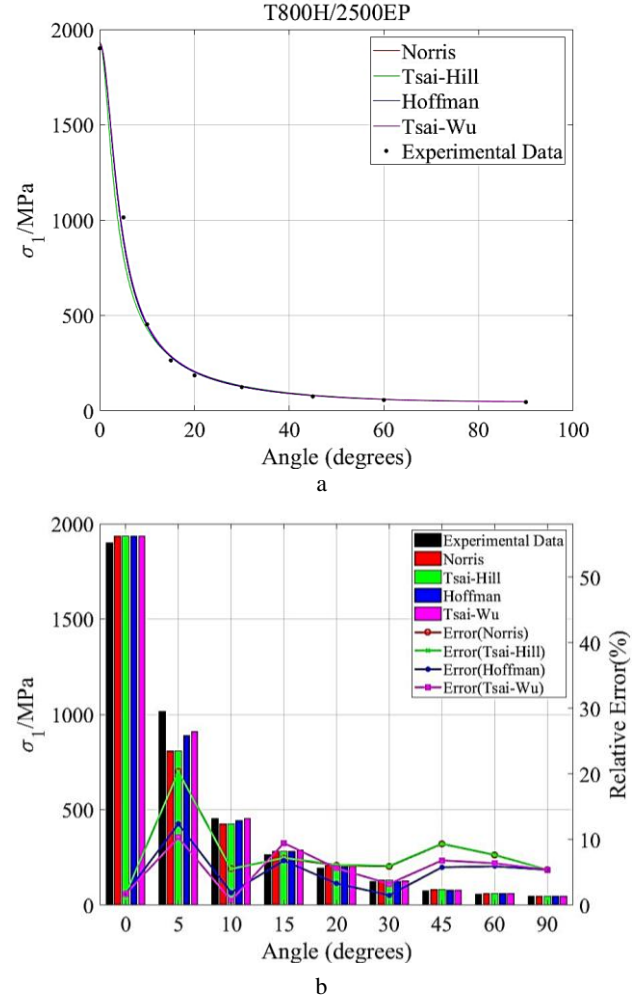


Figure 9 – Comparison of theoretical prediction curves with experimental data: a – approximating curves; b – errors

The data illustrated in Figure 9a indicate that at an off-axis angle of 5°, the experimental values surpass the strengths predicted by theoretical models.

Further analysis, as shown in Figure 9b, reveals that for T800/2500EP laminates, the prediction errors associated with the Norris and Tsai-Hill criteria are greater than those of the Hoffman and Tsai-Wu criteria, with the most significant discrepancy observed at an off-axis angle of 5°.

Pipes and Cole conducted off-axis tensile tests using composite (Boron/AVCO5505) unidirectional plates at six different angles θ (0°, 15°, 30°, 45°, 60°, and 90°).

Figure 10 compares the predicted curves for each criterion and the actual test results. In assessing the tensile strength of the boron/epoxy composites at various off-axis angles, the Norris and Tsai-Hill criteria exhibited more significant prediction errors compared to the Hoffman and Tsai-Wu criteria.

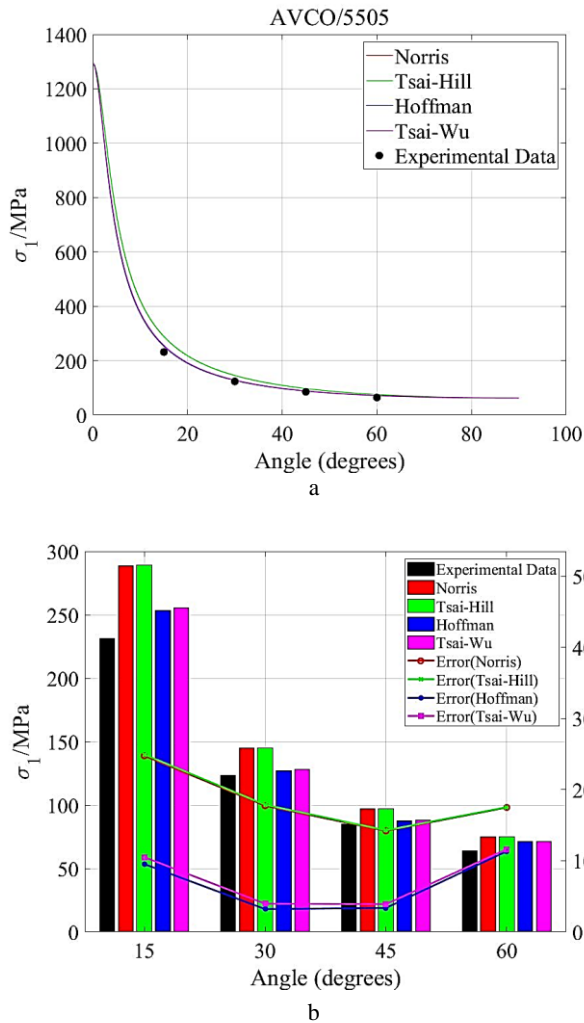


Figure 10 – Comparison of theoretical prediction curves with experimental data: a – approximating curves; b – errors

Notably, the Norris and Tsai-Hill criteria showed the most significant errors at off-axis angles of 15° (24 %) and 60° (17 %). In contrast, the Hoffman and Tsai-Wu criteria demonstrated their most considerable discrepancies at an off-axis angle of 60° , each with an error of 11 %.

In-plane biaxial loading tests constitute a crucial methodology for assessing material responses under multiaxial stress conditions. These tests emulate stress states encountered in practical applications, thereby playing a pivotal role in comprehending and forecasting material behavior. Data collected under varied stress scenarios are instrumental in corroborating the predictive efficacy of the phenomenological strength criterion. Such analyses are vital for elucidating the microscopic mechanisms underpinning material failure, thereby informing material design and engineering strategies to enhance product reliability and safety.

The IM7/8551 test data [22] were used to establish the σ_1 - σ_2 in-plane failure envelope for each strength criterion and analyzed in comparison with the test results for the σ_1 - σ_2 biaxial stress state.

As shown in Figure 11, the Norris and Tsai-Hill criteria are applied considering the different material tensile and

compressive properties, and the corresponding tensile and compressive strengths are used for the tensile and compressive stress states, respectively.

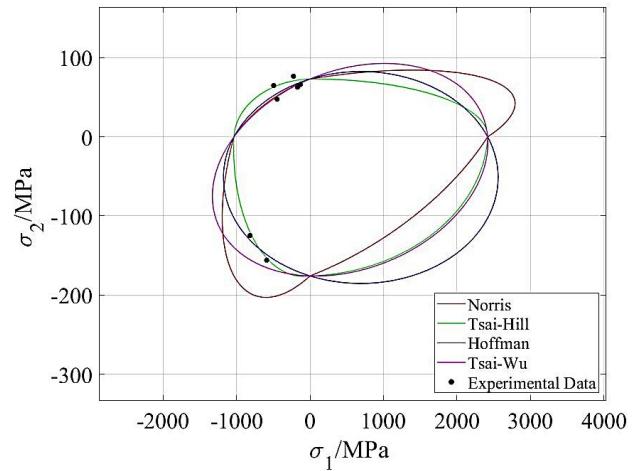


Figure 11 – Comparison of failure envelopes for each strength criterion at σ_1 - σ_2 stress states with experimental data

As can be seen from this figure, in the second quadrant, the prediction results are in better agreement with the test data. In the third quadrant, the prediction curves of Hoffman's criterion agree with the test results, and the deviation of the Norris criterion prediction is the largest.

The test data from T300/BSL914C [23, 24] facilitated the development of σ_1 - τ_{12} in-plane failure envelopes for various strength criteria, which were then compared with the test outcomes under the σ_1 - τ_{12} biaxial stress state, as depicted in Figure 12.

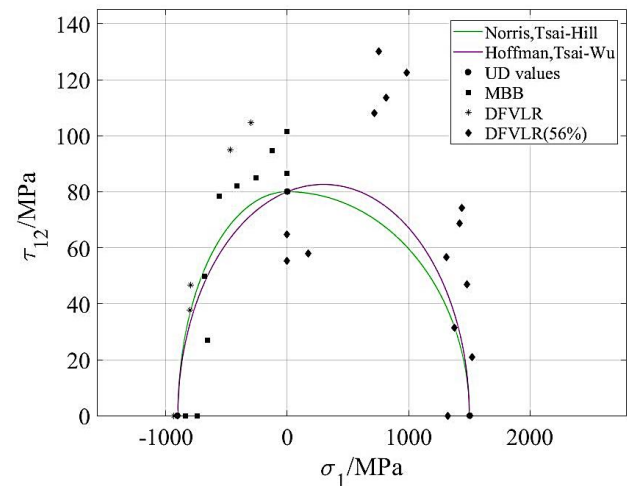


Figure 12 – Comparison of failure envelopes for each strength criterion at σ_1 - τ_{12} stress states with experimental data

Analysis of the figure reveals that the Norris and Tsai-Hill criteria, as well as the Hoffman and Tsai-Wu criteria, exhibit identical expressions and overlapping failure envelopes within the σ_1 - τ_{12} stress state ($\sigma_2 = 0$).

Excluding outlier data, the experimental findings generally align well with the predictions. Specifically, the Norris and Tsai-Hill criteria correlate more closely with

the experimental data in the second quadrant of the σ_1 - τ_{12} stress plane. In contrast, the Hoffman and Tsai-Wu criteria show better alignment in the first quadrant.

The AS4/55A test data [25, 26] were utilized to develop the σ_2 - τ_{12} in-plane failure envelopes for various strength criteria and these were subsequently compared with experimental results under the σ_2 - τ_{12} biaxial stress state. At $\sigma_1 = 0$, the expressions for the Norris criterion, Tsai-Hill criterion, Hoffman criterion, and Tsai-Wu criterion under the σ_2 - τ_{12} stress states are identical, resulting in overlapping failure envelopes.

As illustrated in Figure 13, after excluding anomalous data, it is evident that the failure envelopes for the Norris criterion and Tsai-Hill criterion correspond more closely with experimental findings in the first quadrant of the σ_2 - τ_{12} stress plane.

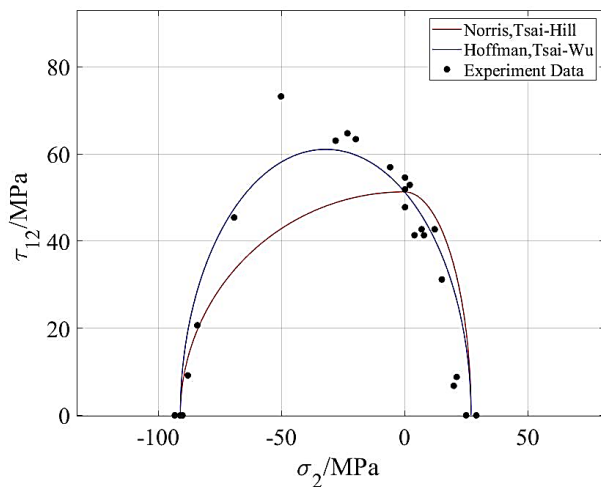


Figure 13 – Comparison of failure envelopes for each strength criterion at σ_2 - τ_{12} stress states with experimental data

Similarly, the Hoffman and Tsai-Wu criteria show better congruence with experimental data in both the first and second quadrants.

5 Discussion

This article presents a comprehensive comparative analysis of the strength criteria of four prevalent composite materials, which differs from previous studies in that it relies not only on experimental and theoretical investigations of single materials but also on comparative analyses of the strength criteria of composite materials. By comparing the off-axis and biaxial test data with the normalized strength criteria, the best use case for each strength criterion is found, and its predictive ability is evaluated.

When discussing the accuracy of strength predictions for composites, comparing these findings with other research results is critical to understanding the reliability and applicability of these guidelines.

In Figures 8–10, the observed differences at specific off-axis angles coincide with the challenges highlighted in the literature regarding the predictive power of

conventional strength codes when applied to complex composites [27, 28].

Also, for example, a similar study [29] reported varying degrees of variability in prediction accuracy between the Norris, Tsai-Hill, Hoffman, and Tsai-Wu codes, which is often attributed to the inherent anisotropy of the material and the complex damage mechanisms of composites in an off-axis stress state.

Furthermore, the significant differences observed in multiaxial in-plane stretching, as shown in Figures 11–13, are consistent with the results of studies highlighting the sensitivity of predicted strength to specific material properties and stress states under consideration [30, 31], further highlighting the subtle nature of composite failure, which is influenced by factors such as load direction, matrix properties, and fiber-matrix interactions [32, 33].

This discussion not only reinforces the view that existing strength guidelines provide valuable tools for predicting the behavior of composites but also highlights the need to carefully assess the applicability of these guidelines in the context of specific material systems and loading conditions, with close attention to empirical validation through experimental data.

Despite their ongoing optimization and reasonable predictive accuracy, the existing phenomenological strength criterion and multiaxial damage model are confined to specific materials and test conditions. However, their applicability and feasibility across varying complex stress scenarios (such as different 2D stress quadrants and 3D stress spaces) require further validation through extensive experimental data to ensure broad applicability and effectiveness. Concurrently, developing more accurate theoretical prediction models remains a valuable endeavor.

6 Conclusions

In this study, we analyzed and evaluated the phenomenological strength theory of composites. Initially, we established a unified form of the phenomenological strength criterion, comparing and analyzing the theoretical envelopes of each criterion. We specifically discussed the impact of varying interaction stress coefficients, F_{12} , on the Tsai-Wu criterion's theoretical envelopes. Utilizing experimental data from existing literature, we plotted the failure envelopes of each strength criterion under a plane combined stress state, elucidating the variations in these envelopes across different stress quadrants. Four representative phenomenological strength criteria were selected for in-depth analysis. Their predictive capabilities were assessed using composite off-axis tensile and biaxial loading test data.

The main findings are as follows. First, the predictions of phenomenological strength theories did not completely and accurately align with all stress state test results. Theoretical predictions varied under different stress states, necessitating the selection of suitable strength criteria and parameters based on specific materials and test results.

Second, under tension, the prediction errors of the Hoffman and Tsai-Wu criteria are higher than those of the

Norris and Tsai-Hill criteria. The Tsai-Wu criterion has the most significant prediction error of 23 % when the off-axis angle $\theta = 15^\circ$. For larger off-axis angles (45° , 60° , and 75°), the prediction error for each criterion was within 20 %.

In the presence of shear, the Norris and Tsai-Hill criteria prediction errors were more significant than those for the Hoffman and Tsai-Wu criteria, with the most significant differences, especially at smaller off-axis angles. The Norris and Tsai-Hill criteria had the most significant errors at an off-axis angle of 15° (24 %) and 60° (17 %), respectively. In contrast, the Hoffman and Tsai-Wu criteria had the most significant error of 11 % at an off-axis angle of 60° .

Finally, in the in-plane biaxial combined stress state, the failure envelopes of each criterion in the IM7/8551 material's $\sigma_1 - \sigma_2$ stress plane's third quadrant were conservative. The Hoffman criterion's predictions closely matched test results, while the Norris criterion showed the most significant deviation. Failure envelopes were

conservative for T300/BSL914C composites in the $\sigma_1 - \tau_{12}$ stress plane. The Norris and Tsai-Hill criteria aligned well with second-quadrant experimental results, and Hoffman and Tsai-Wu criteria matched first-quadrant results.

In the $\sigma_2 - \tau_{12}$ stress plane of AS4/55A composites, Hoffman and Tsai-Wu criteria's failure envelopes aligned well with first quadrant experimental results, being close to Norris and Tsai-Hill's envelopes, which were conservative in the second quadrant.

7 Acknowledgments

The research was funded by the China Scholarship Council. The authors are highly grateful to the colleagues of the Department of Dynamics and Strength of Machines and Strength of the National Technical University of Ukraine "Igor Sikorsky Kyiv Polytechnic Institute, for their cooperation in research activities concerning the development and application of the described methodologies.

References

1. Pyskunov, S., Bakhtavarshoev, T., Samofal, K. (2023). On the use of strength criteria for anisotropic materials. *Strength of Materials and Theory of Structures*, Vol. 110, pp. 496–506. <https://doi.org/10.32347/2410-2547.2023.110.496-506>
2. Forster, E., Clay, S., Holzwarth, R., Paul, D. (2008). Flight vehicle composite structures. In: *The 26th Congress of ICAS and 8th AIAA ATIO. American Institute of Aeronautics and Astronautics*. <https://doi.org/10.2514/6.2008-8976>
3. Tao, F., Liu, X., Du, H., Tian, S., Yu, W. (2022). Discover failure criteria of composites from experimental data by sparse regression. *Composites Part B: Engineering*, Vol. 239, 109947. <https://doi.org/10.1016/j.compositesb.2022.109947>
4. Norris, C. (1962). *Strength of Orthotropic Materials Subjected to Combined Stresses*. Forest Products Laboratory, University of Wisconsin, Madison, WI, USA.
5. Azzi, V. D., Tsai, S. W. (1965). Anisotropic strength of composites. *Experimental Mechanics*, Vol. 5, pp. 283–288. <https://doi.org/10.1007/BF02326292>
6. Hoffman, O. (1967). The brittle strength of orthotropic materials. *Journal of Composite Materials*, Vol. 1, pp. 200–206. <https://doi.org/10.1177/002199836700100210>
7. Tsai, S. W., Wu, E. M. (1971). A general theory of strength for anisotropic materials. *Journal of Composite Materials*, Vol. 5, pp. 58–80. <https://doi.org/10.1177/002199837100500106>
8. Wu, E. M., Scheublein, J. K. (1974). Laminate strength – A direct characterization procedure. *ASTM Special Technical Publications*, Vol. 546, pp. 188–206. <https://doi.org/10.1520/STP35489S>
9. Cowin, S. C. (1979). On the strength anisotropy of bone and wood. *Journal of Applied Mechanics*, Vol. 46(4), pp. 832–838. <https://doi.org/10.1115/1.3424663>
10. Yeh, H.-Y., Kim, C. H. (1994). The Yeh-Stratton criterion for composite materials. *Journal of Composite Materials*, Vol. 28, pp. 926–939. <https://doi.org/10.1177/002199839402801003>
11. Arruda, M. R. T., Almeida-Fernandes, L., Castro, L., Correia, J. R. (2021). Tsai–Wu based orthotropic damage model. *Composites Part C: Open Access*, Vol. 4, 100122. <https://doi.org/10.1016/j.jcomc.2021.100122>
12. Li, S., Xu, M., Sitnikova, E. (2022). The formulation of the quadratic failure criterion for transversely isotropic materials: mathematical and logical considerations. *Journal of Composites Science*, Vol. 6(3), 82. <https://doi.org/10.3390/jcs6030082>
13. Jen, M.-H., Lee, C.-H. (1998). Strength and life in thermoplastic composite laminates under static and fatigue loads. Part I: Experimental. *International Journal of Fatigue*, Vol. 20, pp. 605–615. [https://doi.org/10.1016/S0142-1123\(98\)00029-2](https://doi.org/10.1016/S0142-1123(98)00029-2)
14. Chen, X., Sun, X., Chen, P., Wang, B., Gu, J., Wang, W., Chai, Y., Zhao, Y. (2021). Rationalized improvement of Tsai–Wu failure criterion considering different failure modes of composite materials. *Composite Structures*, Vol. 256, 113120. <https://doi.org/10.1016/j.compstruct.2020.113120>
15. Clouston, P., Lam, F., Barrett, J. D. (1998). Interaction term of Tsai-Wu theory for laminated veneer. *Journal of Materials in Civil Engineering*, Vol. 10, pp. 112–116. [https://doi.org/10.1061/\(ASCE\)0899-1561\(1998\)10:2\(112\)](https://doi.org/10.1061/(ASCE)0899-1561(1998)10:2(112))
16. Evans, K. E., Zhang, W. C. (1987). The determination of the normal interaction term in the Tsai-Wu tensor polynomial strength criterion. *Composites Science and Technology*, Vol. 30, pp. 251–262. [https://doi.org/10.1016/0266-3538\(87\)90014-5](https://doi.org/10.1016/0266-3538(87)90014-5)
17. Groenwold, A. A., Haftka, R. T. (2006). Optimization with non-homogeneous failure criteria like Tsai–Wu for composite laminates. *Structural and Multidisciplinary Optimization*, Vol. 32, pp. 183–190. <https://doi.org/10.1007/s00158-006-0020-3>

18. Li, S., Sitnikova, E., Liang, Y., Kaddour, A.-S. (2017). The Tsai-Wu failure criterion rationalised in the context of UD composites. *Composites Part A: Applied Science and Manufacturing*, Vol. 102, pp. 207–217. <https://doi.org/10.1016/j.compositesa.2017.08.007>
19. Hahn, H. T., Tsai, S. W. (2018). *Introduction to Composite Materials*. CRC Press, Boca Raton, FL, USA.
20. Kawai, M., Yajima, S., Hachinohe, A., Takano, Y. (2001). Off-axis fatigue behavior of unidirectional carbon fiber-reinforced composites at room and high temperatures. *Journal of Composite Materials*, Vol. 35, pp. 545–576. <https://doi.org/10.1177/002199801772662073>
21. Pipes, R. B., Cole, B. W. (1973). On the off-axis strength test for anisotropic materials. *Journal of Composite Materials*, Vol. 7, pp. 246–256. <https://doi.org/10.1177/002199837300700208>
22. Sun, C.-T. (1996). Comparative Evaluation of Failure Analysis Methods for Composite Laminates. National Technical Information Service, Springfield, VA, USA.
23. Soden, P. D., Hinton, M. J., Kaddour, A. S. (2004). Lamina properties, lay-up configurations and loading conditions for a range of fibre-reinforced composite laminates. *Composites Science and Technology*, Vol. 58(7), pp. 1011–1022. [https://doi.org/10.1016/S0266-3538\(98\)00078-5](https://doi.org/10.1016/S0266-3538(98)00078-5)
24. Soden, P. D., Hinton, M. J., Kaddour, A. S. (2004). Biaxial test results for strength and deformation of a range of E-glass and carbon fibre reinforced composite laminates: failure exercise benchmark data. *Composites Science and Technology*, Vol. 62(12–13), pp 1489–1514. [https://doi.org/10.1016/S0266-3538\(02\)00093-3](https://doi.org/10.1016/S0266-3538(02)00093-3)
25. Pinho, S. T., Dávila, C. G., Camanho, P. P., Iannucci, L., Robinson, P. (2005). *Failure Models and Criteria for FRP Under In-Plane or Three-Dimensional Stress States Including Shear Non-Linearity*. NASA Langley Research Center, Hampton, VA, USA.
26. Swanson, S. R., Messick, M. J., Tian, Z. (1987). Failure of carbon/epoxy lamina under combined stress. *Journal of Composite Materials*, Vol. 21, pp. 619–630. <https://doi.org/10.1177/002199838702100703>
27. Hinton, M. J., Kaddour, A. S., Soden, P. D. (2004). A further assessment of the predictive capabilities of current failure theories for composite laminates: Comparison with experimental evidence. *Composites Science and Technology*, Vol. 64(3–4), pp. 549–588. [https://doi.org/10.1016/S0266-3538\(03\)00227-6](https://doi.org/10.1016/S0266-3538(03)00227-6)
28. Tao, F., Liu, X., Du, H., Tian, S., Yu, W. (2022). Discover failure criteria of composites from experimental data by sparse regression. *Composites Part B: Engineering*, Vol. 239, 109947. <https://doi.org/10.1016/j.compositesb.2022.109947>
29. Cai, D., Tang, J., Zhou, G., Wang, X., Li, C., Silberschmidt, V. V. (2017). Failure analysis of plain woven glass/epoxy laminates: Comparison of off-axis and biaxial tension loadings. *Polymer Testing*, Vol. 60, pp. 307–320. <https://doi.org/10.1016/j.polymertesting.2017.04.010>
30. Cai, D., Zhou, G., Wang, X., Li, C., Deng, J. (2017). Experimental investigation on mechanical properties of unidirectional and woven fabric glass/epoxy composites under off-axis tensile loading. *Polymer Testing*, Vol. 58, pp. 142–152. <https://doi.org/10.1016/j.polymertesting.2016.12.023>
31. Zhou, G., Sun, Q., Li, D., Meng, Z., Peng, Y., Zeng, D., Su, X. (2020). Effects of fabric architectures on mechanical and damage behaviors in carbon/epoxy woven composites under multiaxial stress states. *Polymer Testing*, Vol. 90, 106657. <https://doi.org/10.1016/j.polymertesting.2020.106657>
32. Singh, V., Larsson, R., Olsson, R., Marklund, E. (2023). A micromechanics-based model for rate dependent compression loaded unidirectional composites. *Composites Science and Technology*, Vol. 232, 109821. <https://doi.org/10.1016/j.compscitech.2022.109821>
33. Turaka, S., Chintalapudi, R., Geetha, N. K., Pappula, B., Makgato, S. (2024). Experimental and numerical analysis of the microstructure and mechanical properties of unidirectional glass fiber reinforced epoxy composites. *Composite Structures*, Vol. 331, 117887. <https://doi.org/10.1016/j.compstruct.2024.117887>